



# A new approach for the development of diabatic potential energy surfaces: Hybrid block-diagonalization and diabatization by ansatz

Nils Wittenbrink, Florian Venghaus, David M. G. Williams, Wolfgang Eisfeld

## ► To cite this version:

Nils Wittenbrink, Florian Venghaus, David M. G. Williams, Wolfgang Eisfeld. A new approach for the development of diabatic potential energy surfaces: Hybrid block-diagonalization and diabatization by ansatz. *Journal of Chemical Physics*, 2016, 145 (18), pp.184108. 10.1063/1.4967258 . hal-02906093

**HAL Id: hal-02906093**

**<https://hal.science/hal-02906093>**

Submitted on 16 Sep 2022

**HAL** is a multi-disciplinary open access archive for the deposit and dissemination of scientific research documents, whether they are published or not. The documents may come from teaching and research institutions in France or abroad, or from public or private research centers.

L'archive ouverte pluridisciplinaire **HAL**, est destinée au dépôt et à la diffusion de documents scientifiques de niveau recherche, publiés ou non, émanant des établissements d'enseignement et de recherche français ou étrangers, des laboratoires publics ou privés.

# A new approach for the development of diabatic potential energy surfaces: Hybrid block-diagonalization and diabatization by *ansatz*

Cite as: J. Chem. Phys. **145**, 184108 (2016); <https://doi.org/10.1063/1.4967258>

Submitted: 11 July 2016 • Accepted: 25 October 2016 • Published Online: 11 November 2016

Nils Wittenbrink, Florian Venghaus, David Williams, et al.



View Online



Export Citation



CrossMark

## ARTICLES YOU MAY BE INTERESTED IN

**Neural network diabatization: A new ansatz for accurate high-dimensional coupled potential energy surfaces**

The Journal of Chemical Physics **149**, 204106 (2018); <https://doi.org/10.1063/1.5053664>

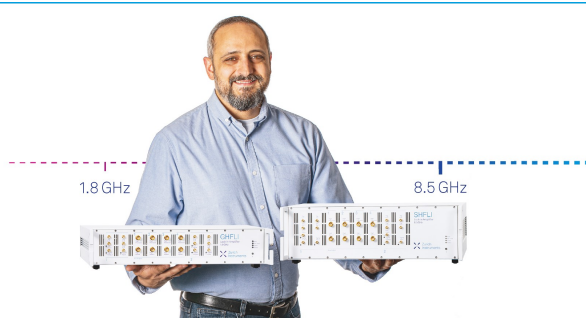
**Block-diagonalization as a tool for the robust diabatization of high-dimensional potential energy surfaces**

The Journal of Chemical Physics **144**, 114110 (2016); <https://doi.org/10.1063/1.4943869>

**Approximately diabatic states from block diagonalization of the electronic Hamiltonian**


The Journal of Chemical Physics **89**, 7367 (1988); <https://doi.org/10.1063/1.455268>





**Trailblazers.** New

Meet the Lock-in Amplifiers that measure microwaves.

 Zurich Instruments [Find out more](#)

# A new approach for the development of diabatic potential energy surfaces: Hybrid block-diagonalization and diabaticization by *ansatz*

Nils Wittenbrink, Florian Venghaus, David Williams, and Wolfgang Eisfeld<sup>a)</sup>

*Theoretische Chemie, Universität Bielefeld, Postfach 100131, D-33501 Bielefeld, Germany*

(Received 11 July 2016; accepted 25 October 2016; published online 11 November 2016)

A new diabaticization method is presented, which is suitable for the development of accurate high-dimensional coupled potential energy surfaces for use in quantum dynamics studies. The method is based on the simultaneous use of adiabatic wave function and energy data, respectively, and combines block-diagonalization and diabaticization by *ansatz* approaches. It thus is called hybrid diabaticization. The adiabatic wave functions of suitable *ab initio* calculations are projected onto a diabatic state space and the resulting vectors are orthonormalized like in standard block-diagonalization. A parametrized diabatic model Hamiltonian is set up as an *ansatz* for which the block-diagonalization data can be utilized to find the optimal model. Finally, the parameters are optimized with respect to the *ab initio* reference data such that the deviations between adiabatic energies and eigenvalues of the model as well as projected state vectors and eigenvectors of the model are minimized. This approach is particularly advantageous for problems with a complicated electronic structure where the diabatic state space must be of higher dimension than the number of calculated adiabatic states. This is an efficient way to handle problems with intruder states, which are very common for reactive systems. The use of wave function information also increases the information content for each data point without additional cost, which is beneficial in handling the undersampling problem for high-dimensional systems. The new method and its performance are demonstrated by application to three prototypical systems, ozone ( $\text{O}_3$ ), methyl iodide ( $\text{CH}_3\text{I}$ ), and propargyl ( $\text{H}_2\text{CCCH}$ ). *Published by AIP Publishing*. [<http://dx.doi.org/10.1063/1.4967258>]

## I. INTRODUCTION

The detailed study of reactive processes at molecular level is of fundamental interest for understanding chemistry. The tremendous progress in experimental techniques provides a plethora of data and the great advance in theory can deliver the corresponding interpretations to gain deep insight. However, the complexity of the experimental data and the effort for a theoretical treatment of a reactive process increase extremely rapidly with the size of the system. One of the main theoretical bottlenecks for systems beyond three atoms is the development of accurate analytical potential energy surfaces (PESs), which are essential for a theoretical (quantum) reaction dynamics investigation. At least for adiabatic ground states, two strategies have proven feasible for developing higher-dimensional PESs with good accuracy. One possibility is based on local interpolation techniques<sup>1–5</sup> while the other utilizes invariant theory and permutation symmetry of indistinguishable nuclei.<sup>6</sup> A third approach is currently emerging with promising results, which is based on artificial neural networks.<sup>7–24</sup> Unfortunately, an extension of these methods to excited state PESs is not straightforward because of the difficulty to account for the state-state interactions. So far, this has been attempted by the modified Shepard interpolation<sup>25–27</sup> and very recently by using invariant polynomials and complete nuclear permutation-inversion (CNPI) symmetry.<sup>28,29</sup>

For excited states, it generally is of great advantage to use a *quasi*-diabatic representation for the coupled electronic states.<sup>30–43</sup> A unique and truly diabatic representation in general cannot be defined strictly and it might be better to speak of a *quasi*-diabatic representation.<sup>37,43</sup> In the following we will still use the term “diabatic” rather than “*quasi*-diabatic” simply for the convenience of the reader. The requirement for a suitable diabatic representation is that it minimizes the remaining derivative coupling among the states in the model and the states not included into the model to a degree that it can be neglected like in the standard Born-Oppenheimer approximation.<sup>43</sup> Most attempts to develop coupled PESs for a manifold of states are based on some kind of diabatic representation. This simplifies the quantum dynamics treatment because the diabaticization removes the singularities of the nonadiabatic derivative couplings. Furthermore, the matrix elements of the electronic Hamiltonian become particularly simple functions in a diabatic basis, making it easier to find analytical expressions for them.

One of the simplest approaches of this kind is the linear vibronic coupling model, which has been an early and extremely successful approach for the explanation of many phenomena in ultra fast nuclear dynamics.<sup>44</sup> Unfortunately, the standard linear vibronic coupling model is only useful for describing processes that are entirely dominated by the short-time dynamics so that only a very small part of the coupled potential energy surfaces (PESs) is of importance. However, we are interested in processes that are not of this kind

<sup>a)</sup>wolfgang.eisfeld@uni-bielefeld.de

and require accurate PESs over extended regions of nuclear configurations. For this reason we and others have been extending the vibronic coupling approach in recent work.<sup>39,45–51</sup> The advantage of the vibronic coupling approach and the corresponding “diabatization by *ansatz*” technique is that it yields directly a PES matrix in closed form. The disadvantage is that in the absence of high molecular symmetry there might be a fair amount of ambiguity in the diabatization because only adiabatic electronic energies are used and no information about the electronic wave functions is utilized.

Some early diabatization approaches used properties of the wave functions rather than the energies for the diabatization.<sup>36,52</sup> Related to these ideas was the development of wave function based direct diabatization schemes. An early version of this kind of approach was introduced by Cimraglia *et al.*<sup>53</sup> who defined a set of asymptotic diabatic reference states with respect to which the wave functions at all other geometries are diabatized within an *ab initio* code to directly compute diabatic states and energies. The method is based on unitary transformations of the states to fulfill maximal overlap criteria combined with the use of quasi-degenerate perturbation theory. A lot of scientific effort has been devoted to similar techniques by which diabatic energies and nonadiabatic couplings can be determined from the electronic wave functions within the framework of electronic structure methods.<sup>54–66</sup> In general, the direct diabatization approaches do not yield analytic PES matrices directly. Some of these methods compute and annihilate the nonadiabatic coupling elements and are thus reference-free while others are based on a reference point. The approaches annihilating the nonadiabatic couplings benefited strongly from the advent of analytic evaluation techniques of the derivative couplings within the framework of multiconfiguration-reference configuration interaction (MRCI).<sup>67</sup> For example, the diabatization algorithm of Nakamura and Truhlar<sup>58</sup> is based on the generation of diabatic molecular orbitals (DMOs) and characteristic configuration state functions (CSFs) in the basis of those DMOs. This procedure yields diabatic wave functions, energies, and nonadiabatic couplings in an automatic way and was extended to also account for the atomic spin-orbit (SO) coupling matrix.<sup>68</sup> The advantage of such methods is that the diabatization model is generated more or less automatically. By point-wise computation of the diabatic properties, a PES model might be constructed subsequently. In principle, all these methods are based on the ideas of block-diagonalization of the electronic Hamiltonian.<sup>40</sup> The applicability of such methods for the construction of diabatic PESs has been demonstrated by Domcke *et al.* who developed a particularly simple approach.<sup>54,55</sup> They used their method to determine a diabatic two-state PES model for ozone, properly describing the conical intersection of the  $^1A_2$  and  $^1B_1$  states.<sup>69</sup> This model will also be used as a reference test case in the present work.

We recently developed a new method for the generation of SO coupled diabatic PESs based on analytic atomic SO coupling matrices and a special kind of diabatization.<sup>70–72</sup> The central idea is a diabatic representation of the spin-space (“spin-free”) adiabatic states with a reference point at the atom-fragment asymptote and thus the method is called Effective Relativistic Coupling by Asymptotic Representation

(ERCAR). The method requires that all states corresponding to a specific atom-fragment asymptotic state need to be represented throughout the nuclear configuration space. However, some of these states may be ionic or otherwise become very high in energy, meaning that it is unfeasible to compute *ab initio* electronic structure energy reference data for them to determine the model parameters. On the other hand, only low-lying adiabatic states are relevant for the dynamics of most processes of interest. Thus, it is sufficient to determine the diabatic representation of these high-energy states only from the adiabatic wave functions using the block-diagonalization ideas and without the need of energy data. We combine this approach with a “diabatization by *ansatz*” to represent the more relevant states in order to obtain highly accurate PESs for them with a reliable representation of the adiabatic wave functions as well.

In the present work we extend these ideas to a general approach of a hybrid diabatization by *ansatz* and block-diagonalization method. In the following we will present the theoretical background and the details of the method, followed by some applications to demonstrate the power of the approach and the accuracy of the PESs obtained.

## II. THEORY

### A. Adiabatic and diabatic representations

The typical approach to handle the complicated problem of a molecular quantum system is to separate the total Hamiltonian

$$\hat{H}(\mathbf{q}, \mathbf{Q}) = \hat{H}_{nn}(\mathbf{Q}) + \hat{H}_{ne}(\mathbf{q}, \mathbf{Q}) + \hat{H}_{ee}(\mathbf{q}) \quad (1)$$

into the part that only depends on the nuclear coordinates  $\mathbf{Q}$  and the remaining electronic Hamiltonian

$$\hat{H}_{el}(\mathbf{q}, \mathbf{Q}) = \hat{H}_{ne}(\mathbf{q}, \mathbf{Q}) + \hat{H}_{ee}(\mathbf{q}), \quad (2)$$

which depends on both nuclear coordinates  $\mathbf{Q}$  and electronic coordinates  $\mathbf{q}$ . Eq. (2) may be solved approximately for any given nuclear configuration  $\mathbf{Q}$  using modern electronic structure methods. The electronic eigenenergy  $E_j^a(\mathbf{Q})$  corresponding to the  $j$ th eigenstate  $|\psi_j^a(\mathbf{q}; \mathbf{Q})\rangle$  of Eq. (2) defines the  $j$ th adiabatic PES of the system. The adiabatic state  $|\psi_j^a\rangle$  is defined by being an eigenstate of  $\hat{H}_{el}$  for any given nuclear configuration  $\mathbf{Q}$ . Thus, the total Hamiltonian can be expressed in the adiabatic representation as

$$\hat{H}^a(\mathbf{q}, \mathbf{Q}) = \hat{H}_{nn}(\mathbf{Q}) \mathbf{1} + \hat{\Lambda}(\mathbf{Q}) + E^a(\mathbf{Q}), \quad (3)$$

where the electronic degrees of freedom have been integrated out resulting in the adiabatic potential matrix  $E^a$ . As is well known, the nuclear kinetic energy operator in  $\hat{H}_{nn}$  induces a nonadiabatic or derivative coupling  $\hat{\Lambda}$  among the adiabatic states that may become troublesome in regions where the coupling gets strong. The idea of a diabatic basis is that the diabatic states forming this basis are chosen such that the derivative coupling is reduced to a degree that it can be neglected safely. The price to pay is that diabatic states in general are not eigenstates of  $\hat{H}_{el}$  anymore and that a diabatic basis cannot be defined without ambiguity and arbitrariness.

The diabatic states belong to  $\hat{H}_{el}$  and thus the adiabatic states can be expanded in terms of the diabatic basis as

$$|\psi_j^a\rangle = \sum_k u_{kj} |\psi_k^d\rangle. \quad (4)$$

The evaluation of the matrix elements of  $\hat{H}_{el}$ ,

$$\langle \psi_i^a | H_{el} | \psi_j^a \rangle = \sum_{k,l} u_{ki}^* u_{lj} \langle \psi_k^d | H_{el} | \psi_l^d \rangle = \sum_{k,l} u_{ki}^* u_{lj} w_{kl}^d(\mathbf{Q}), \quad (5)$$

yields the diabatic potential matrix  $\mathbf{W}^d$ . If both adiabatic and diabatic basis were complete, the expansion coefficients  $u_{kj}$  would correspond exactly to the elements of the unitary transformation matrix that diagonalizes  $\mathbf{W}^d$  to yield the adiabatic state energies  $E_j^a$  as eigenvalues according to

$$\mathbf{U}^\dagger \mathbf{W}^d \mathbf{U} = \mathbf{E}^a = \text{diag}(E_j^a). \quad (6)$$

This relation is crucial for the diabatization approach presented in the following.

## B. Group Born-Oppenheimer approximation

No approximations have been introduced up to this point because we have assumed that both adiabatic and diabatic bases are complete. Of course, any reasonable state basis for the electronic problem is far from complete and for any practical application only a small number of states can be handled. Typically, it is possible to find a small subset of adiabatic states among which nonadiabatic couplings are important, while the interactions to all other states are small enough to be neglected. The reasoning here is the same as the one used in the usual adiabatic or Born-Oppenheimer approximation. The only difference is that in the present case a group of states is separated from all others by neglecting the corresponding nonadiabatic couplings. This is called the group Born-Oppenheimer approximation.<sup>30</sup>

Let us assume that we want to treat a limited number of  $N^a$  adiabatic states and omit any further states by invoking the group Born-Oppenheimer approximation. We represent each of the  $N^a$  adiabatic states in a finite  $N^d$ -dimensional diabatic basis by

$$|\psi_j^a\rangle \approx \sum_{k=1}^{N^d} u_{kj} |\psi_k^d\rangle, \quad j = 1, \dots, N^a, \quad N^d \geq N^a, \quad (7)$$

which now is only an approximate representation due to the limitation of the chosen basis. While in many diabatization approaches the dimension of the diabatic basis is equal to the number of adiabatic states of interest, this is not a requirement for the present method. In fact, the hybrid diabatization was developed especially for the case where  $N^d > N^a$  due to the particular choice of diabatic states as required for the representation of relativistic couplings.<sup>70–72</sup> More generally, different diabatic basis states are important in different areas of nuclear configuration space, which means that a diabatization with  $N^d > N^a$  usually is necessary for global diabatic PES models. Furthermore, the eigenvalues of the finite diabatic potential matrix,  $E_j^d(\mathbf{Q})$ , will also show deviations from the exact adiabatic PESs,  $E_j^a(\mathbf{Q})$ . A larger diabatic basis reduces these deviations and improves the accuracy of representing the

adiabatic PESs by the diabatic potential matrix. The explicit choice of the diabatic basis will be explained below.

## C. Adiabatic states from *ab initio* calculations

In order to obtain a diabatic model for a set of coupled PESs, one first needs to compute adiabatic energies and wave functions for the electronic states of interest. Special attention has to be paid to the representation of the adiabatic wave functions as was first pointed out by Woywod and Domcke.<sup>54,55</sup> First of all, we want to express the adiabatic states in terms of configuration state functions (CSFs) as

$$|\psi_j^a(\mathbf{q}; \mathbf{Q})\rangle = \sum_{k=1}^M c_{kj}(\mathbf{Q}) |\psi_k^{CSF}(\mathbf{q}; \mathbf{Q})\rangle \quad (8)$$

with the number of CSFs,  $M$ , being much larger than  $N^d$ . It is of great advantage to use CASSCF wave functions optimized for the set of electronic states of interest. The active molecular orbitals from the CASSCF calculations are not unique because within the active space all pairwise orbital rotations are redundant and the CASSCF energy is invariant. Therefore, it is necessary to diabatize the CASSCF MOs first before the corresponding CI vectors can be used for an analysis of the electronic wave functions. This diabatization of the MOs can be achieved in various ways.<sup>54–56,58,73</sup> In the present study we use the simple method by Woywod and Domcke that is based on maximizing the overlap of the current CASSCF MOs with a set of reference orbitals precomputed for a specific nuclear geometry. After the MOs are diabatized in this way and the CASSCF CI vectors are transformed into the diabatic orbital basis, the resulting CI coefficients  $c_{kj}$  can be related directly to the expansion coefficients  $u_{kj}$  in terms of diabatic states, Eq. (7). Instead of the CASSCF CI vectors, also CI vectors from higher level calculations like MRCI can be used for that purpose. The idea behind this is that a diabatic state can be defined as one that preserves its character upon changes of the nuclear coordinates and this character can be associated with a single CSF or a fixed linear combination of CSFs. This concept is known as preservation of configurational uniformity<sup>56,73</sup> and has been applied in various diabatization approaches.<sup>39,40,53,58,59,74–77</sup> This means that for a given set of adiabatic states one can easily find the required set of diabatic basis states by analyzing the major contributions of CSFs to the *ab initio* CI vectors when moving through nuclear configuration space. The corresponding CI coefficients in principle provide sufficient information to diabatize the adiabatic energies in the spirit of the various block-diagonalization approaches.<sup>40,54,55,58,59,73,77</sup> However, this will not yield the diabatic potential matrix directly, which is the goal of the present work. In the following it will be shown how this can be achieved by combining the information of the CI coefficients with an explicit diabatic potential model.

## D. Diabatic model (*ansatz*)

As was pointed out in the discussion of Eq. (6), the connection between the diabatic and adiabatic potential matrices is the basis transformation that diagonalizes the diabatic matrix for any given nuclear configuration. What remains is a representation of the diabatic matrix elements in closed mathematical



form. Since the diabatic states by definition are slowly varying functions of the nuclear coordinates, the same will be true for the diabatic matrix elements. In fact, it has been shown that such slowly varying functions are a sufficient condition for the minimization of the remaining derivative coupling mentioned in Sec. I.<sup>30,43</sup> As a result, the matrix elements can be expressed by very simple functions of the nuclear coordinates. In principle, any type of parametrized function could be used as long as basic requirements as symmetry properties are fulfilled. For simplicity, they can be expanded as parametrized multi-dimensional polynomials

$$w_{kl}^d(\mathbf{Q}) = \sum_a p_a^{kl} \prod_b Q_b^{n_{ab}^{kl}} \quad (9)$$

in terms of a suitable set of nuclear coordinates  $Q_b$ . The choice of these coordinates often is important for the accuracy and may account for symmetry, asymptotic behaviour, etc. The expansion coefficients  $p_a^{kl}$  are parameters which have to be determined based on the *ab initio* data (see below). In the most general form, one can use all products of powers  $n_{ab}^{kl}$  of coordinates  $Q_b$  up to a certain order  $o_a^{kl} = \sum_b n_{ab}^{kl}$  for each term for a given matrix element. However, it usually is better to use more sophisticated choices for the polynomial expansion, selecting specific multi-mode terms and powers as needed to optimally reproduce the adiabatic *ab initio* reference data. Furthermore, the symmetry of the system may require that certain parameters vanish while other parameters might be related to each other by fixed ratios determined by group theory.<sup>44,46,47,78,79</sup> A typical example for this situation would be a Jahn-Teller state with a symmetry-induced conical intersection. Such conditions should be utilized *a priori* for the method to be efficient and reliable. The analysis of the *ab initio* CI vectors also helps to determine which diabatic coupling elements are of significance and which elements may be set to zero or can be approximated at a lower level than the more important matrix elements.<sup>80</sup> This will be discussed in more detail for the specific examples in Section III.

## E. Hybrid diabaticization

A sufficient condition for diabaticizing the adiabatic reference data would be that, once the diabatic model is defined, the free parameters are determined such that the diabatic eigenvalues reproduce the adiabatic energies sufficiently well throughout the nuclear configuration space. This entirely energy-based approach is called diabaticization by *ansatz* and is being used extensively for vibronic coupling problems.<sup>44</sup> The strength of this method is to model a very limited region of the PESs by a low-order expansion, which is sufficient for short-time dynamics of ultra-fast processes. However, for the accurate representation of larger regions of the PESs, one generally has to expand the diabatic matrix to higher orders and the diabaticization by *ansatz* may become rather troublesome. For this reason, we developed the present hybrid approach, which combines the diabaticization by *ansatz* with the use of wave function information as in the previously discussed block-diagonalization methods.

For this purpose, a subspace of the selected CSFs that correspond to diabatic states is defined as described above.

Diabatic states can also be defined by fixed orthonormalized linear combinations of CSFs of the selected subspace. Then the CI coefficients corresponding to this subspace are collected for each relevant adiabatic state for all nuclear configurations of the reference data set. The corresponding CI vectors for each nuclear configuration  $\mathbf{Q}$  are projected onto the diabatic basis vectors. This defines a set of subspace CI vectors,  $\mathbf{c}_j^{\text{sub}}(\mathbf{Q})$ , in which the CI coefficients are ordered according to the diabatic basis as defined by the diabatic potential matrix. The dimension  $N^{\text{sub}}$  of the  $\mathbf{c}_j^{\text{sub}}$  vectors is much smaller than  $M$  so that a symmetric reorthonormalization procedure is required, which is shown below.

In the first step, the subspace CI vectors  $\mathbf{c}_j^{\text{sub}}(\mathbf{Q})$  are renormalized by

$$\tilde{\mathbf{c}}_j(\mathbf{Q}) = \frac{\mathbf{c}_j^{\text{sub}}(\mathbf{Q})}{\|\mathbf{c}_j^{\text{sub}}(\mathbf{Q})\|}. \quad (10)$$

The renormalized CI vectors  $\tilde{\mathbf{c}}_j(\mathbf{Q})$  are then used to form the square matrix  $\mathbf{S}(\mathbf{Q})$  with matrix elements

$$S_{jk}(\mathbf{Q}) = \tilde{\mathbf{c}}_j^\dagger(\mathbf{Q}) \cdot \tilde{\mathbf{c}}_k(\mathbf{Q}), \quad (11)$$

which corresponds to an overlap matrix. This is a real, symmetric, positive semi-definite matrix and thus can be diagonalized by

$$\mathbf{s}(\mathbf{Q}) = \text{diag}(\mathbf{s}_j(\mathbf{Q})) = \mathbf{V}^\dagger(\mathbf{Q}) \mathbf{S}(\mathbf{Q}) \mathbf{V}(\mathbf{Q}), \quad (12)$$

yielding the eigenvalues  $s_j$ . Eigenvalues of zero would correspond to linearly dependent state vectors  $\tilde{\mathbf{c}}_j$ , which can be ruled out. Therefore, the real matrix  $\mathbf{s}^{-\frac{1}{2}}$  can be formed containing the inverse square-roots of the eigenvalues of  $\mathbf{S}$ . This matrix is then used to construct the transformation matrix  $\mathbf{T}$  obtained from the back transformation of  $\mathbf{s}^{-\frac{1}{2}}$  by

$$\mathbf{T}(\mathbf{Q}) = \mathbf{V}(\mathbf{Q}) \mathbf{s}^{-\frac{1}{2}}(\mathbf{Q}) \mathbf{V}^\dagger(\mathbf{Q}). \quad (13)$$

The matrix  $\mathbf{T}(\mathbf{Q})$  is finally used to generate orthonormal CI vectors  $\mathbf{c}_j^{\text{on}}(\mathbf{Q})$  as the column vectors of the matrix

$$\mathbf{C}^{\text{on}}(\mathbf{Q}) = \tilde{\mathbf{C}}(\mathbf{Q}) \mathbf{T}(\mathbf{Q}), \quad (14)$$

which are used for the fitting process. The entries  $c_{kj}^{\text{on}}$  correspond directly to the expansion coefficient of the  $k$ th diabatic basis state for the  $j$ th adiabatic state. This procedure essentially is the well-known symmetric reorthogonalization applied to the projected CI vectors in the space spanned by the diabatic basis vectors. This is equivalent to the orthogonalization of AO basis functions in electronic structure, e.g., in typical Hartree-Fock methods (see, e.g., Ref. 81).

One big advantage of the hybrid diabaticization over traditional block-diagonalization techniques is that phase information can be neglected. Only the phase-free CI weights

$$d_{kj}(\mathbf{Q}) = |c_{kj}^{\text{on}}(\mathbf{Q})|^2 \quad (15)$$

are needed and computed by taking the absolute square of the symmetrically renormalized subspace vector components. The CI weights are sufficient for the hybrid diabaticization because this approach is based on non-linear least-squares fitting, minimizing a penalty function  $f(\mathbf{p})$  that can be defined at will (see below). Of course, one could also use the CI vectors if the phase relations are standardized in some way.

The CI weights correspond directly to the contribution of the respective diabatic state to the adiabatic wave function in question. For each nuclear configuration  $\mathbf{Q}$  we have  $N^a$  adiabatic energies and  $N^a \times N^{sub}$  CI weights as reference data from the *ab initio* calculations in order to determine the free parameters of the diabatic model. Of course, one usually wants to determine the adiabatic energies with the best accuracy possible, which means that CASSCF most likely is insufficient. It is straightforward to replace the CASSCF energies by the results from advanced correlation treatments like MRCI, CASPT2, or maybe even MR-CC calculations. The CI coefficients can also be taken from advanced MRCI or similar calculations. The number of total possible configurations  $M$  increases dramatically, but the number of the resulting CI weights stays constant after projection and the symmetric reorthonormalization.

Finally, the actual determination of the optimal parameters  $\mathbf{p}$  of the diabatic matrix is carried out by least-squares fitting. This requires the definition of a penalty function,  $f(\mathbf{p})$ , which is to be minimized. The penalty function for the hybrid diabatization using CI weights reads

$$f(\mathbf{p}) = \sum_i \sum_j^{N^a} \rho_{ij} \left( E_j^a(\mathbf{Q}_i) - E_j^d(\mathbf{Q}_i; \mathbf{p}) \right)^2 + \sum_k^{N^{sub}} \sigma_{ijk} \left( d_{jk}(\mathbf{Q}_i) - u_{jk}(\mathbf{Q}_i; \mathbf{p}) \right)^2 \rightarrow \min \quad (16)$$

in which the first sum runs over all nuclear configurations  $\mathbf{Q}_i$  in the *ab initio* data set,  $\rho_{ij}$  are fitting weights for the adiabatic energies, and  $\sigma_{ijk}$  are fitting weights for the CI configuration weights. In principle, the mixing of different physical properties in this particular function, energies, and wave function information, adds an element of ambiguity. However, exactly the inclusion of wave function data to an otherwise energy based diabatization procedure enforces a physically meaningful diabatization result, especially when using very flexible *ansatz* functions for the diabatic matrix elements. Special attention has to be paid to the  $\rho_{ij}$  and  $\sigma_{ijk}$  fitting weights because the significance of the squared errors of energies and CI weights may be vastly different. For example, if the reference energies are given in atomic units, an acceptable deviation might be of the order of  $10^{-5}$ – $10^{-6}$ . By contrast, a deviation in the state composition of 1% for a given diabatic basis state would correspond to  $10^{-2}$ – $10^{-3}$  and thus would contribute orders of magnitude more to the penalty function than an energy deviation of  $10 \mu E_h$  if the fitting weights were equal. A further effect to be taken into account is that there are  $N^{sub}$  times more input data for the CI weights than for the adiabatic energies. This problem can be solved by a simple scaling like

$$\sigma_{ijk} = \frac{\phi_{ij}^E}{N^{sub} \phi_{ijk}^d} \rho_{ij} \sigma_{ijk}^{in} \quad (17)$$

in which  $\phi_{ij}^E$  is the acceptable error for energy deviations and  $\phi_{ijk}^d$  is the acceptable deviation in state composition. The multiplication with the input fitting weight  $\sigma_{ijk}^{in}$  allows for further flexibility in the fitting procedure. The  $\rho_{ij}$  fitting weights for

the adiabatic energies can be adapted to the required accuracy in various regions of the PESs, e.g., by energy criteria or manual manipulation as is frequently used in PES fitting.

The actual minimization of the penalty function can be carried out by any suitable standard optimization method. The only limitation is that the diagonalization of the diabatic matrix is required in order to obtain the energies  $E_j^d(\mathbf{Q}_i)$ , which renders the problem non-linear. In our present implementation we use a dual-layer approach of standard Marquardt-Levenberg fitting embedded into a genetic algorithm. Starting from an initial guess for the parameters, the genetic algorithm stochastically generates trial parameter sets, which are then used as input for the Marquardt-Levenberg optimization. Then a limited number of new parent sets is selected based on the obtained fitting errors. The next generation of trial parameter sets is generated by scrambling the parent sets and additional mutations. Usually the optimization converges within fairly few generations and the parameter set giving the smallest root mean square (rms) error is selected as the final result.

## F. Practical aspects

The hybrid diabatization method, which is described above, is a versatile and powerful method for the construction of diabatic PESs. Still, certain aspects have to be taken into account in order to achieve accurate results. One of the most important challenges is the generation of consistent electronic structure data. Especially when treating systems undergoing dissociation, it is very difficult to find an appropriate active orbital and state space, which is closed throughout the nuclear configuration space. During the set up of the *ab initio* calculations, problems with active/inactive orbital rotations and intruder states have to be identified and solved to guarantee reference data that can be diabatized. For a detailed description of methods to analyse and fix such problems, we refer to our recent work regarding block-diagonalization.<sup>80</sup>

Second, a good starting guess is necessary for the cumbersome non-linear fitting procedure. It has been shown that decoupling the system via block-diagonalization and fitting all matrix elements independently from each other offers a reliable path to generate starting guesses systematically. Additionally, from the block-diagonalization one can get detailed information on the matrix elements, which helps a lot in setting up the model. By analyzing the shape of the diagonal and off-diagonal elements in advance, appropriate forms of the *ansatz* can be chosen and very small off-diagonal elements can be neglected and set to zero. After that analysis, the matrix elements can be fitted linearly or non-linearly (depending on the *ansatz*) and independently from each other.

The hybrid diabatization as described above requires several steps of analysis, data gathering, data manipulation, model set up, and numerical fitting. The entire procedure is summarized in a flow chart visualising the sequence of necessary steps for the generation of a set of diabatic PESs using the hybrid diabatization method (Figure 1).

## III. APPLICATIONS

The previously described hybrid diabatization method will be demonstrated in the following by application to various

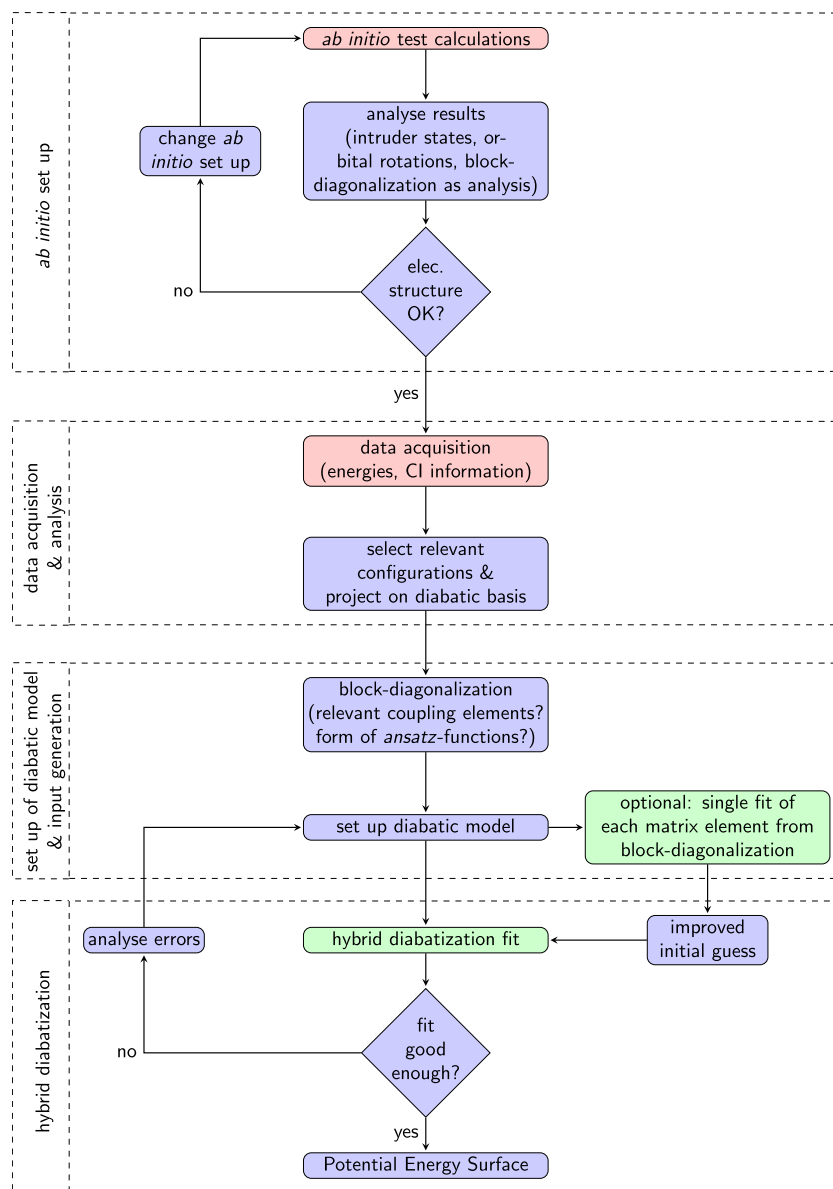


FIG. 1. Flowchart visualising all steps of the hybrid diabatization method. Red boxes are *ab initio* calculations, green boxes are (non-linear) fitting procedures, and blue boxes are several different types of data analysis and model preparing. The loops are necessary to ensure an optimal model with minimal deviation in the final PES and might be passed a few times.

systems to show the performance and flexibility of the method and the accuracy of the fitting results.

A simple proof-of-principle example is the conical intersection of two electronic states of the ozone ( $\text{O}_3$ ) molecule which has been investigated by Woywod and Domcke<sup>54,55</sup> and others.<sup>73</sup> For this rather simple system with only two electronic states, the applicability and accuracy of the new hybrid diabatization method are shown in general.

The methyl iodide ( $\text{CH}_3\text{I}$ ) system is a more complicated example where the dynamics of the photodissociation is of interest. Bond breaking occurs and needs to be described accurately by the PESs. In the present example, we only focus on the dissociation coordinate and keep the methyl fragment fixed. The electronic structure changes heavily upon the C–I bond breaking and different states and orbitals are important in different areas of the PESs. Highly excited states, which cannot be calculated via standard *ab initio* techniques, are relevant

in this case<sup>70–72</sup> and their treatment by the hybrid diabatization method is demonstrated. A stable diabatization is ensured because it is possible to treat all kinds of conical intersections and intruder states observed in the optimized *ab initio* treatment of the reference data.<sup>80</sup>

Finally the highly complex propargyl radical ( $\text{H}-\text{C}-\text{C}-\text{CH}_2$ ) is treated by hybrid diabatization. Using this challenging 12-dimensional example with many excited states and complicated electronic structure, the full power of the new diabatization technique is demonstrated. For this system we mostly focus on the bound state region of the full-dimensional, coupled PESs in order to simulate the absorption spectra.

## A. Ozone

The conical intersection of the  $^1\text{A}_2$  and the  $^1\text{B}_1$  electronic state has been used as a test case for diabatization previously



by Woywod and Domcke<sup>54,55</sup> on a CASSCF level of theory. This simple two state model is used here as a proof-of-principle example. Therefore, the same setup of the underlying *ab initio* calculations is used for the hybrid diabaticization model as was reported by Domcke and co-workers.

### 1. Symmetry and coordinates

Utilizing the symmetry of a system usually is of great advantage. Therefore, symmetry displacement coordinates relative to a reference point in  $C_{2v}$ -symmetry are used to represent the diabatic matrix. Starting from the primitive valence distances  $r_1$ ,  $r_2$  and the bonding angle  $\alpha$ , linear combination leads to a set of coordinates transforming like irreducible representations  $a_1$  and  $b_2$  of  $C_{2v}$ .

As a reference point for the diabaticization the bonding angle of the conical intersection  $\alpha = 120.942^\circ$  with a ground state equilibrium distance of  $r_{1,2} = 1.296 \text{ \AA}$  is chosen. For this proof-of-principle model, we only treat displacements in the asymmetric stretch coordinate  $r_c = r_1 - r_2$  and the bending coordinate  $\alpha$ , which are of  $b_2$  and  $a_1$  symmetry, respectively. *Ab initio* data were calculated for 1271 geometries in an area from  $r_c = -0.4 \text{ \AA}$  to  $0.4 \text{ \AA}$  and  $\alpha = 90^\circ$ – $150^\circ$ .

It needs to be mentioned that the ozone system shows strong multi-reference character. Four different configurations play an important role in the area described above. Therefore, the CI vectors from the *ab initio* data were projected onto the reference vectors of the diabatic basis states defined at the conical intersection in the basis of the four relevant CSFs. The resulting projected CI vectors then only consist of the two components corresponding to the two different diabatic reference states.

### 2. Diabatic model

The symmetry properties of the displaced coordinates described above are important in setting up a model for the diabatic matrix  $\mathbf{W}^d$ . Each diagonal matrix element  $w_{ii}^d$  has to transform like  $a_1$  and the off-diagonal matrix element  $w_{12}^d$  needs to transform like  $b_2$  to ensure the correct symmetry of the total Hamiltonian. The matrix is expanded in polynomials in the displacement coordinates  $r_c$  and  $\alpha$ , which yields product terms of the form  $\alpha^k r_c^l$ . Thus non-zero matrix elements  $w_{ii}^d$  only contain even exponents  $l$  and non-zero matrix elements  $w_{12}^d$  only contain odd exponents  $l$ . In this work, the polynomials are expanded up to an order of  $N = 6$ . Altogether, the *ansatz* for the diabatic matrix  $\mathbf{W}^d$  can be written as

$$W_{ii}^d(\alpha, r_c) = \sum_{j,k}^{j+2k=N} p_{jk}^{ii} \alpha^j r_c^{2k}, \quad (18)$$

$$W_{12}^d(\alpha, r_c) = \sum_{j,k}^{j+2k+1=N} p_{jk}^{12} \alpha^j r_c^{2k+1}, \quad (19)$$

with parameters  $p_{jk}$  which have to be determined by an appropriate fitting procedure.

### 3. Fitting weights

The advantage of the new hybrid diabaticization method is that both *ab initio* energies and CI vectors are used for the

fitting procedure. As described in Eq. (16), the fitting weights must be balanced to ensure the best possible fit result. The fitting weights  $\rho_{ij}$  of the adiabatic energies are scaled with an exponential decay

$$\rho_{ij} = \exp\left(-3\left(E_j^a(\mathbf{Q}_i) - E_j^a(\mathbf{Q}_0)\right)\right). \quad (20)$$

This renders the lower energies at the conical intersection and near the potential minimum more important than higher energies which is a sensible choice because *ab initio* data can be problematic for higher energies where further couplings to states not included in the model can occur. To account for the different orders of magnitude between energies and CI coefficients, the further scaling of the fitting weights for the CI coefficients follows

$$\sigma_{ijk}(d_{jk}) = \gamma \cdot \rho_{ij} \cdot (1 - 0.9d_{jk}). \quad (21)$$

The pre-factor  $\gamma$  is chosen as 0.01 for the ozone system. Once all fitting weights are determined, a non-linear Marquardt-Levenberg minimization embedded in a genetic algorithm is used to find the optimal parameters for the diabatic model.

### 4. Accuracy of hybrid diabaticization

The fits were calculated for total orders  $N = 2, 4, 6$  of the diabatic model. Figure 2 shows the fit results compared to the reference data, which immediately illustrates that the second order expansion is not sufficient to describe the PESs even qualitatively. The potential minimum and the area around the conical intersection are not reproduced properly. The higher order expansions obviously perform better and seem to follow the underlying *ab initio* data perfectly. A quantitative view on the results is shown in Table I. The fourth order expansion already yields quite accurate results but still results in a noticeable error in the energies, which is about an order of magnitude larger than the error for the sixth order. The errors with respect to the state composition are already very small for the fourth order fit and are improved only slightly by the sixth order fit. The squared elements of the first projected CI vector are displayed in the two right panels of Figure 2 and are compared to *ab initio* values. The sudden exchange of the values in the top panel is a signature of a scan passing through a conical intersection at which point the two eigenvectors simply switch. The gradual exchange of the vectors observed in the bottom panel is typical for an avoided crossing, nicely showing the extended region of nonadiabatic state interaction and thus significant mixing of the two diabatic state components.

To verify the fit result and to check that enough *ab initio* data points have been used, further data points are calculated along random vectors in the 2D configuration space which are not included in the fit. Figure 3 shows a selection of random scans in comparison to the diabatic model, demonstrating the quality of the diabatic representation. The rms deviation of the *ab initio* data from the random scans in comparison to the fitting result is  $3.9 \text{ cm}^{-1}$ , which is similar to the rms error of the data used to optimize the parameters. This proves that the number of data points is sufficient and the model is highly accurate.

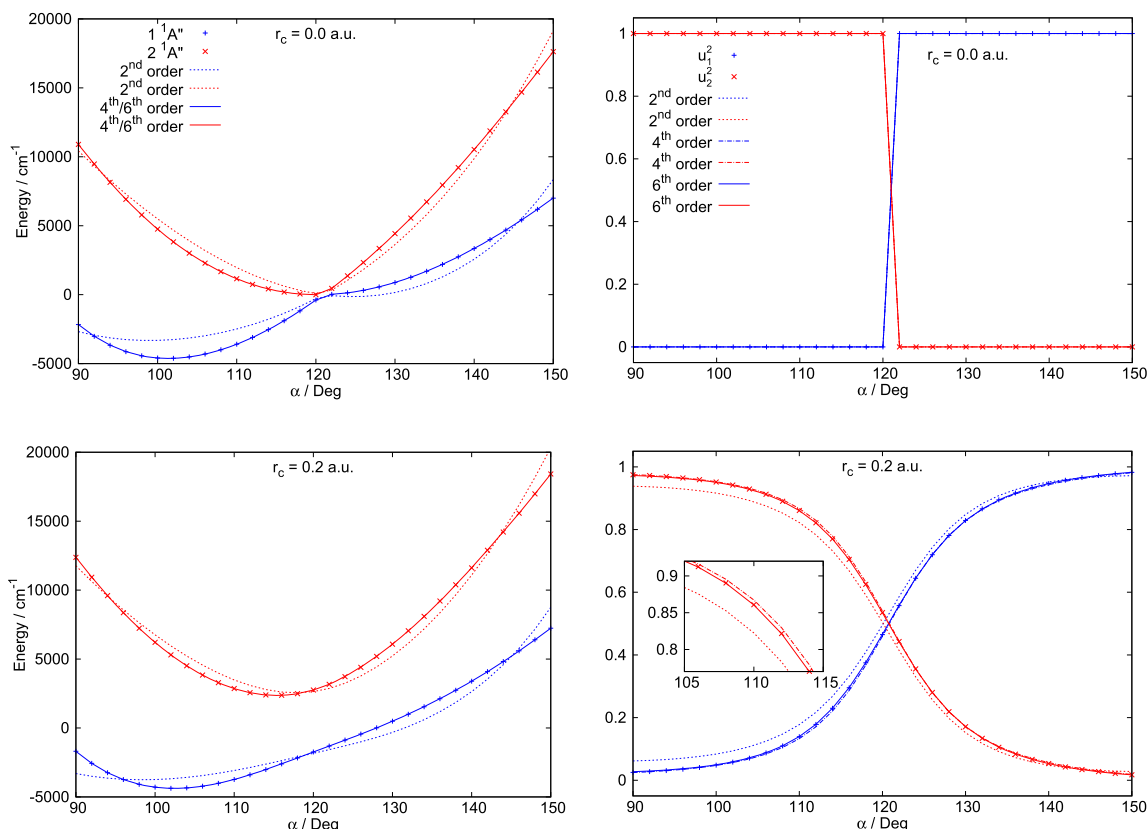


FIG. 2. On the left, 1D-cuts through the PESs of ozone for different distances  $r_c = r_1 - r_2$  and result of the hybrid diabaticization for 2nd, 4th, and 6th order are shown. Single points are adiabatic *ab initio* reference data and straight lines are eigenvalues of the diabatic model. Plots for 4th and 6th order are indistinguishable at scale of plot, thus only one line is drawn for both. On the right, squared elements of the eigenvectors of the hybrid diabaticization model and squared elements of the *ab initio* CI vectors are shown.

## B. Methyl iodide

The photodissociation of methyl iodide is an example for ultra-fast dynamics including conical intersections induced by spin-orbit coupling. After the rather simple two state model for ozone, the methyl iodide system as the second example is much more complicated. The specific strength of the hybrid diabaticization method in describing states not directly accessible over the complete nuclear configuration space via *ab initio* methods is highlighted by the methyl iodide system.

### 1. Electronic structure

For an accurate description of the photo dissociation, many excited states need to be calculated over a large region of the nuclear configuration space. Here, the C–I dissociation coordinate is treated as a first step where several conical

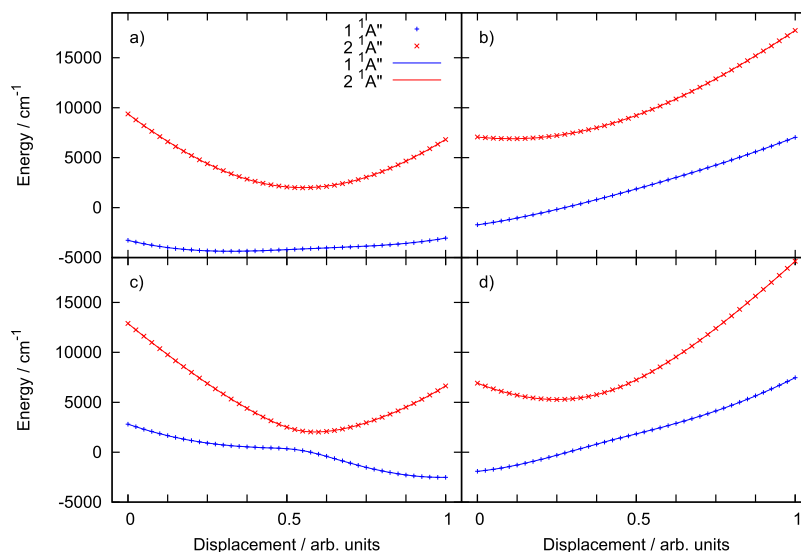
intersections, avoided crossings, and other changes in the electronic structure occur. To ensure consistency of the *ab initio* data for the full dimensional surfaces, all calculations are carried out without any symmetry restriction on the electronic wave functions. The underlying data of this work are obtained by the Molpro code<sup>82</sup> using CASSCF and internally contracted multiconfiguration-reference configuration interaction (MRCI).<sup>83,84</sup> 7 singlet and 6 triplet states are calculated along the C–I dissociation coordinate with distances between 1.6 and 20 Å. The full technical details of the *ab initio* calculations are given elsewhere.<sup>72</sup> During our previous studies on the ERCAR model,<sup>70–72</sup> it was shown that it is necessary to use many high-lying states in the diabatic model to accurately represent the spin-orbit coupling. Depending on the C–I distance, these high-lying states may or may not be among the 7, respectively, 6 adiabatic states computed *ab initio*. It is not possible to represent these states reasonably in the model using standard block-diagonalization or diabaticization by *ansatz* procedures. Hybrid diabaticization on the other hand is the perfect tool for this task because high-lying states can be described in the diabatic model without explicitly calculating them *ab initio*. The necessary data are encoded in the projected CI vectors of the available adiabatic states.

### 2. Diabatic model for CH<sub>3</sub>I

The diabatic model for CH<sub>3</sub>I is meant to be used within the ERCAR method to represent the spin-orbit coupled diabatic

TABLE I. Errors (rms) of the eigenvalues of the diabatic model vs. *ab initio* adiabatic energies for different order  $N$  of the expansion of the diabatic model of ozone. Additionally, the rms error in the state composition is shown.

Order $N$	Energy (cm <sup>-1</sup> )	Composition (%)
2	893.9	3.28
4	45.5	0.41
6	4.1	0.23

FIG. 3. Comparison of the *ab initio* data of the four random scans vs. hybrid diabaticization model energies of ozone.

PESs of the fine structure states. This requires an asymptotic diabatic basis of direct product states of atomic iodine and molecular methyl states.

For an accurate description of the spin-orbit coupling effects in the iodine atom, both the  $5s^25p^5$  ground state electronic configuration and the  $5s^25p^46s^1$  excited states configuration have to be taken into account. The ground state configuration only corresponds to a  $^2P$  state, whereas the excited electron configuration corresponds to four different spin-space states ( $^4P$ ,  $2^2P$ ,  $^2D$ , and  $^2S$ ). Positively charged iodine states with a  $5s^25p^4$  electronic configuration ( $^3P$ ,  $^1S$ , and  $^1D$ ) and negatively charged states with a  $5s^25p^6$  ( $^1S$ ) and  $5s^25p^56s^1$  ( $^1P$  and  $^3P$ ) configuration arise from ionic separation of the fragments. Combination with the methyl fragment in the electronic ground states ( $^2A_2''$  and  $^1A_1'$ ) yields a total number of 100 fine structure direct product states. A list of all states with corresponding symmetries and the number of fine structure state components is given in Table II.

Standard *ab initio* electronic structure methods are far from being able to calculate accurate energies for this huge

number of states. Depending on the region of the nuclear configuration space, only a few of these states are within reach of these calculations. Furthermore, the dissociation along the C–I coordinate obviously causes drastic changes of the electronic structure. Thus, the consistency of the underlying *ab initio* calculations has to be ensured first, which has been achieved by techniques developed by us very recently utilizing the block-diagonalization.<sup>80</sup>

When describing bond dissociation, there will always remain certain challenges with the unclosed state space. Electronic states which are of low energy at the dissociation limit will be of high energy in the bonding region and are not covered by the *ab initio* calculations there. A schematic representation of such states is shown in Figure 4. Assume a CASSCF calculation with two states (circles and squares) which should be represented by a model. The ground state (circles) is smooth along the entire dissociation coordinate whereas the excited adiabatic state (squares) shows a conical intersection or avoided crossing. This situation can be described if two different diabatic states are used to represent the one excited adiabatic state of interest. Thus, altogether three diabatic

TABLE II. List of all fine structure basis states contributing to the spin-orbit model for iodine with symmetry labels in  $C_{3v}$ .

Iodine		CH <sub>3</sub>	Symmetries in $C_{3v}$	Number
I ( $^1P$ )	⊗	CH <sub>3</sub> ( $^2A_2''$ )	$^1A_1, ^1E, 3A_1, ^3E$	12
I ( $^4P$ )	⊗	CH <sub>3</sub> ( $^2A_2''$ )	$^3A_2, ^3E, ^5A_2, ^5E$	24
I ( $2^2P$ )	⊗	CH <sub>3</sub> ( $^2A_2''$ )	$^1A_2, ^1E, ^3A_2, ^3E$	12
I ( $^2D$ )	⊗	CH <sub>3</sub> ( $^2A_1'$ )	$^1A_1, 2^1E, ^3A_1, 2^3E$	20
I ( $^2S$ )	⊗	CH <sub>3</sub> ( $^2A_1'$ )	$^1A_1, ^3A_1$	4
I <sup>+</sup> ( $^1S$ )	⊗	CH <sub>3</sub> <sup>+</sup> ( $^1A_1'$ )	$^1A_1$	1
I <sup>+</sup> ( $^3P$ )	⊗	CH <sub>3</sub> <sup>+</sup> ( $^1A_1'$ )	$^3A_1, ^3E$	9
I <sup>+</sup> ( $^1P$ )	⊗	CH <sub>3</sub> <sup>+</sup> ( $^1A_1'$ )	$^1A_1, ^1E$	3
I <sup>+</sup> ( $^3P$ )	⊗	CH <sub>3</sub> <sup>−</sup> ( $^1A_1'$ )	$^3A_2, ^3E$	9
I <sup>+</sup> ( $^1D$ )	⊗	CH <sub>3</sub> <sup>−</sup> ( $^1A_1'$ )	$^1A_1, 2^1E$	5
I <sup>+</sup> ( $^1S$ )	⊗	CH <sub>3</sub> <sup>−</sup> ( $^1A_1'$ )	$^1A_1$	1

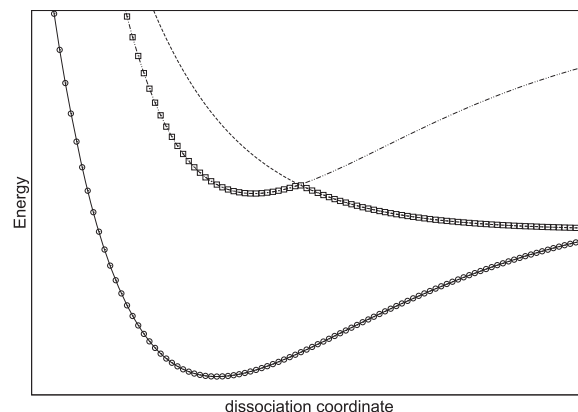


FIG. 4. Scheme of an intruder state coming down for a larger dissociation coordinate.

states are necessary to model the two adiabatic states of Figure 4.

Block-diagonalization techniques are not capable of diabatizing these states accurately and consistently along the coordinate because the number of adiabatic states  $N^a$  and the number of diabatic states  $N^d$  must be equal. Therefore, one would need to calculate another adiabatic state, which is both more expensive and likely to produce even more problems in other regions of the nuclear configuration space, if it is possible at all. Hybrid diabatization on the contrary can treat cases with  $N^d > N^a$  in the same way as described above in Section II. In the example of Figure 4 the diabatic basis would consist of three states and each of the two adiabatic states is expressed in this basis, reflected by the 3-dimensional projected subspace CI vectors. Thus, the required data for the third diabatic state at each point are contained in the two adiabatic subspace CI vectors.

For the case of methyl iodide that means that a diabatic model for the required  $7^1A_1$  spin space states can be set up with only two or three adiabatic states. States of other symmetries can also be described with only a few adiabatic states. As long as the system remains in  $C_{3v}$  symmetry, states corresponding to different irreducible representations can be treated separately.

### 3. Approximate block-diagonalization

To get a first insight into the diabatic states of methyl iodide along the C–I dissociation coordinate, an approximate block-diagonalization method is used. In general, the symmetric diabatic potential matrices  $\mathbf{W}^d$  consist of  $\frac{n(n+1)}{2}$  unique matrix elements, which describe the diabatic coupling among all  $n$  states. This large amount of matrix elements which need to be represented by a model can be reduced drastically if certain off-diagonal elements or couplings can be neglected beforehand. For the analysis, the diagonal adiabatic matrix  $\mathbf{E}^a$  is transformed pointwise with the CI-matrix  $\mathbf{C}^{\text{on}}$  obtained from the *ab initio* calculations and block-diagonalization,

$$\mathbf{W}^d = \mathbf{C}^{\text{on}} \mathbf{E}^a \mathbf{C}^{\text{on}\dagger}. \quad (22)$$

Having a closer view at Eq. (22) immediately reveals problems in the case of  $N^d \neq N^a$ . Straightforward block-diagonalization is not possible in that case because of different dimensions of matrices  $\mathbf{W}^d$  and  $\mathbf{E}^a$ . In order to still use block-diagonalization as a tool for analysis, it must be ensured that the number of adiabatic energies equals the necessary number of diabatic states. One option is to add roughly estimated model data for missing energies and the other is to use additional *ab initio* data if possible, e.g., from more approximate calculations. In this work, we set up additional *ab initio* calculations for that purpose. 22 singlet, 21 triplet, and 3 quintet states are calculated by a small CI calculation with a restricted number of configurations. Only the configurations representing the necessary states in Table II are allowed for the excitations. These calculations yield inaccurate energies because of the reduced CI space and thus a poor description of dynamic electron correlation. But no intruder states can occur since all states possible within this configuration space are computed. Data from these low level *ab initio* calculations are then treated like the accurate data. After symmetric reorthonormalisation the resulting CI vectors and adiabatic energies can be used in Eq. (22).

For this rough model it is possible to look at all matrix elements  $w_{ij}^d$  independently of each other. Figure 5 shows the 21 off-diagonal coupling elements between the seven diabatic states of  $^1A_1$  symmetry as an example. It is obvious at first glance that several of the off-diagonal elements are close to zero nearly for the complete dissociation coordinate and thus are irrelevant. Others only contribute little to the coupling and also may be neglected in the diabatic model. Only a reduced number of couplings is necessary, which reduces the computational cost for the fitting of the diabatic model considerably. In case of the  $^1A_1$  symmetry, a reduction from 21 to 14 relevant coupling elements is achieved.

A second advantage of this preliminary block-diagonalization prior to the full diabatization is that information about the shape and thus mathematical form of the diabatic energies and off-diagonal elements can be extracted and a physically sensible *ansatz* can be obtained. In the case of  $\text{CH}_3\text{I}$ , it is obvious that all diabatic energies have to become constant for large distances between iodine and the fixed methyl fragment. The off-diagonal coupling elements have to vanish for large distances. Still, there needs to be flexibility in the area of interaction between the nuclei. An adequate choice for the representation of the matrix elements  $w_{ij}^d$  for both repulsive and bound states, which also treats the long distance interaction of ions correctly, is

$$w_{ij}^d(r) = p_0^{ij} + \frac{p_1^{ij}}{r} + \sum_{k=2}^6 \frac{p_k^{ij}}{r^{2k}} + p_7^{ij} e^{-p_8^{ij} r}. \quad (23)$$

The parameters  $p_1^{ij}$  can be fixed at zero for all off-diagonal coupling elements and also for diagonal elements if the fragments of the dissociation are not charged. Additionally, the parameters  $p_0^{ij}$  have fixed values. For off-diagonal matrix elements, they are zero, because the states do not couple at infinite C–I distance and the diagonal diabatic elements are determined by the values of atomic iodine energies. The other parameters  $p_k^{ij}$  need to be determined via fitting algorithms. In contrast to straight diabatization by *ansatz* techniques, the matrix elements  $w_{ij}^d$  of the block-diagonalization data can be fitted independently from each other. The non-linear fitting

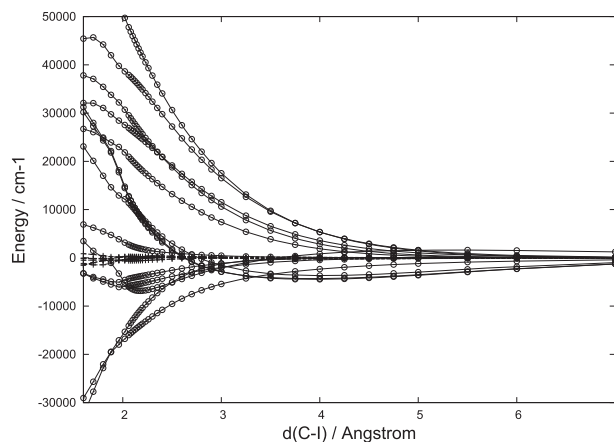


FIG. 5. Off-diagonal diabatic matrix elements of symmetry  $^1A_1$ . The dashed lines represent matrix elements close to zero and are neglected in the diabatic model, solid lines represent relevant matrix elements included into the model, open circles and crosses are *ab initio* block-diagonalization data.



of uncoupled single matrix elements is relatively easy and straightforward using the *ansatz* described above in Eq. (23). For the diagonal elements  $w_{ii}^d$  which refer to diabatic energies, the asymptotic energy  $p_0^{ij}$  is fixed to the energy of the corresponding iodine atomic state in Table II. The remaining seven parameters for states corresponding to homolytic dissociation or eight parameters for heterolytic dissociation are then freely relaxed with a Marquardt-Levenberg algorithm embedded in a genetic algorithm. The merged results of the fitting procedure for all diagonal elements are shown in Figure 6 and corresponding rms errors of all matrix elements are given in Table III.

This example shows that all diabatic matrix elements can be represented at least qualitatively by the chosen *ansatz*. Still, the vastly varying rms errors among different states already show certain limitations of this *block-diagonalization only* model. This is due to the fact that one has no possibility to control or even balance the fit among the different matrix elements, which are all fitted independently from each other. Diagonalization of the diabatic matrix  $\mathbf{W}^d$  yields the adiabatic energies as eigenvalues, which could be compared directly with the *ab initio* data. However, since we used inaccurate model data as underlying *ab initio* data, such a comparison is of no interest because it does not refer to the accurate *ab initio* data. The main advantage of the fitted data from the block-diagonalization is that the obtained set of parameters  $p_k^{ij}$  can be used as a starting guess for the coupled hybrid diabatization fit and it helps in setting up the model at the beginning.

#### 4. Fitting weights

One of the most important parts in setting up a hybrid diabatization model is a sensible choice of the fitting weights. The general setup of the fitting weights for methyl iodide is similar to the previously described one for ozone. Because many high-lying states are present in this model, the decay of the weights with increasing energy is increased and reads

$$\rho_{ij} = \exp \left( -5 \left( E_j^a(\mathbf{Q}_i) - E_j^a(\mathbf{Q}_0) \right) \right). \quad (24)$$

As described in the theory section in Eq. (17), attention has to be paid to the balance between energy weights and CI weights.

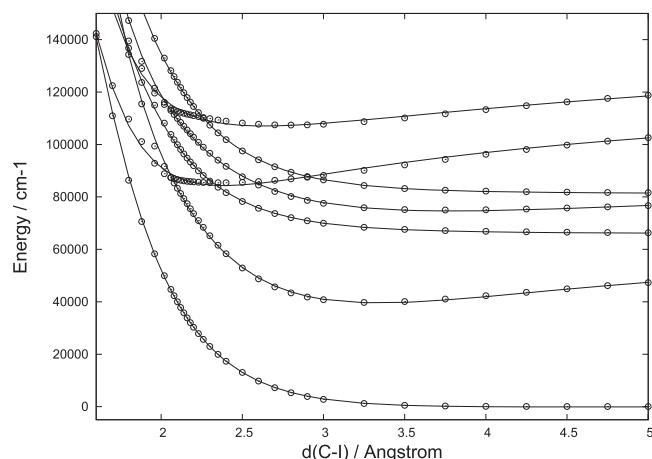


FIG. 6. Fit of block-diagonalized diabatic energies of symmetry  $^1A_1$ . Solid lines are diabatic energies from the model, open circles are *ab initio* block-diagonalization data.

TABLE III. Unweighted rms error in  $\text{cm}^{-1}$  of matrix elements for the  $^1A_1$  states after block diagonalization and fitting.

Element	rms/ $\text{cm}^{-1}$
1-1	275.3
2-2	754.2
3-3	715.7
4-4	1109.1
5-5	701.8
6-6	907.0
7-7	1128.0
1-2	68.6
1-3	86.8
1-4	198.9
1-5	207.2
1-6	201.1
1-7	92.6
2-3	123.8
2-5	144.6
2-6	396.6
3-5	152.6
3-7	433.4
4-5	484.4
4-7	92.8
6-7	124.9

In addition to the scaling of the weights depending on the energy and the issues discussed for ozone, the weights for the CI coefficients are scaled with the number of states  $N$  in the diabatic system. The total weight for CI coefficients is chosen as

$$\sigma_{ijk}(N) = \frac{\gamma_j \cdot \rho_{ij} \cdot (1 - 0.9d_{jk})}{N} \quad (25)$$

with a pre-factor  $\gamma_j = 0.05$  for the lowest energy state and a pre-factor of  $\gamma_j = 0.005$  for all other states. A comparison of fitting results with different pre-factors  $\gamma$  is discussed below. This weighting scheme has shown to be powerful and flexible, which fulfills our needs to construct accurate PESs. Still, manual manipulation of the fitting weights can be necessary and useful in certain areas of the PESs.

#### 5. Accuracy of the results

The results of the hybrid diabatization fit using the fitting weights described above and the block-diagonalization data as a starting guess are shown in Figure 7. The performance of the hybrid diabatization is excellent for this example, particularly when compared to block-diagonalization. The fitting errors of the adiabatic energies from hybrid diabatization are one to two orders of magnitude smaller than those obtained from the pure block-diagonalization as described in Section III B 3. A closer look at the region of the avoided crossing between states 2 and 3 is given in Figure 8 demonstrating the quality of the hybrid diabatization fit. All features of the PESs are reproduced very well and the energy rms errors (Table IV) of the low-lying states show excellent quantitative agreement. Naturally, the rms error is slightly higher for states with strong diabatic coupling like the  $^3A_1$  state. Also the composition of the adiabatic states is in excellent agreement with the *ab initio* data.



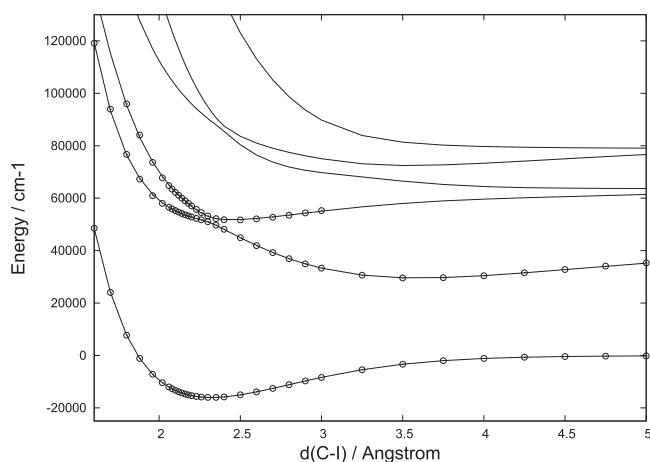


FIG. 7. Result of hybrid diabaticization fit with starting parameters taken from block-diagonalization of symmetry  $^1A_1$ . Solid lines are eigenvalues of the diabatic model, open circles are *ab initio* reference energies.

Results of hybrid diabaticization fits are given for different pre-factors  $\gamma$  in Table IV. One of the main advantages of the hybrid diabaticization method becomes obvious there. By adjusting the  $\gamma$ -parameter, the accuracy can be balanced between energy and state composition depending on the treated system. A relatively high value of  $\gamma$  is necessary for CI-dependent models like ERCAR. For  $\gamma = 0$  no CI information is included in the model and the hybrid diabaticization reduces to the well-known diabaticization by *ansatz*. In the present case the energy errors can be improved noticeably by reducing  $\gamma$  from 0.1 to 0.01. At the same time the deviations in the CI coefficients increases only very slightly.

### C. Propargyl

The last and most complex example demonstrating the power of our new approach is the propargyl radical. The 12 degrees of freedom of this system greatly affect the development of the PESs, rendering this a very challenging task. One of the major effects is essentially independent of diabaticization. Due to the large number of coordinates for high-dimensional systems, the representation of the complete nuclear configuration space quickly becomes problematic. Since not only the

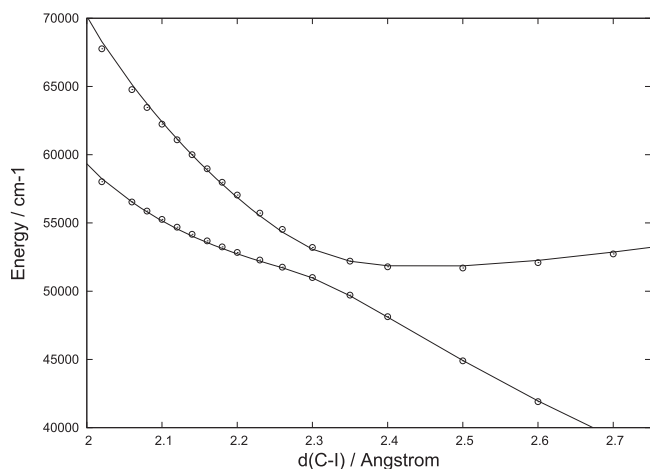


FIG. 8. Closer view of the avoided crossing of the  $^1A_1$  symmetry. The result of hybrid diabaticization is shown in solid lines, open circles are *ab initio* data.

TABLE IV. Unweighted rms errors of the lowest energy states of hybrid diabaticization results for all symmetries depending on the pre-factor for the weight-scaling. The left number in each column is the rms error of the energy in  $\text{cm}^{-1}$  and the right one is the rms error of the state composition in %.

Symmetry	$\gamma$					
	0.1		0.05		0.01	
$^1A_1$	10.1	0.5	9.6	0.3	9.1	0.6
$^1E$	25.7	1.4	31.9	1.5	7.9	1.9
$^3A_1$	40.6	0.6	26.9	0.9	22.5	0.8
$^3E$	17.3	0.6	14.5	0.8	7.2	0.7

required number of data points but also the required computation time for each point increases rapidly with the system size, this quickly evolves into an undersampling problem, for which no obvious solution is available. Another effect more directly connected to diabaticization is the size of the diabatic model and the number of free parameters optimized in the non-linear fit. This number is directly related to the number of states and, more importantly, the number of possible coordinate combinations, rapidly becoming the main contributor in this regard. For the propargyl radical, the hybrid diabaticization is used to target these well-known problems in several ways. On the one hand, the use of the wave function information helps to determine an optimal diabatic model and thus allows to represent the diabatic Hamiltonian by a minimum of necessary parameters. On the other hand, the great information content of both adiabatic energies and wave functions may reduce the effects of undersampling and assists in the determination of a large number of free parameters. Even though the sampling of nuclear configurations must be very sparse, the requirement to reproduce the adiabatic wave functions puts much stricter restrictions on the parameters and thus may enforce that a reasonable representation of the Hamiltonian in a wider region around the actual nuclear configuration is achieved.

### 1. Electronic structure

The electronic structure of the propargyl radical has been found to be rather complicated.<sup>80,85,86</sup> Many effects like orbital rotations or incomplete state spaces can lead to problems. These issues also have considerable effects on the quality of a diabaticization. Therefore, it is of great interest to analyse the electronic structure and see if the *ab initio* data are suitable for diabaticization at all. First, the information obtained by the block-diagonalization is used to find a stable electronic structure. We have reported the details of such an analysis and the corresponding theoretical background very recently.<sup>80</sup>

The reference data needed for the hybrid-diabaticization in the form of the adiabatic energies and adiabatic wavefunctions have been calculated with the Molpro *ab initio* suite of codes using the MRCI method.<sup>82–84</sup> These calculations include 9 electronic states, which are determined along a large number of 12D random vectors. The full technical details of the *ab initio* calculations are given elsewhere.<sup>80</sup> Analysis of the final *ab initio* data shows that it is advantageous to perform the hybrid diabaticization with an additional virtual state. This is performed in the same manner as discussed above in the case of methyl iodide and greatly increases the accuracy of the fit.

## 2. Diabatic model

The construction of the diabatic model for propargyl follows a generic scheme utilizing the system's symmetry and general matrix elements of the form of Eq. (9). However, the generic approach still includes a lot of arbitrariness regarding the order of the respective matrix elements of the diabatic model matrix. Especially in this example with 12 coordinates, 9 adiabatic and 10 diabatic states, respectively, a systematic analysis of specific coupling elements would be a very tedious task and in many cases not worth the trouble. Thus, a more general way to determine the diabatic model has been chosen.

Like in the example of methyl iodide, the data obtained by the block-diagonalization are used to find a physically motivated diabatic model. In this regard, the diabatic matrix elements from the block-diagonalization are analysed in terms of significance and complexity to estimate a suitable approximation. The specific procedure is also described in our previous work and thus will not be repeated here.<sup>80</sup> In addition to this analysis, the symmetry requirements for the diabatic Hamiltonian are utilized, which has to transform as the totally symmetric irreducible representation of the molecular symmetry transformation group. In the case of propargyl, we use the  $C_{2v}$  point group since proton exchange is unlikely to be relevant in our applications. Combined with symmetrized coordinates, this helps to reduce the diabatic matrix even further and allows for a comparably simple diabatic model. The diabatic model used in the examples shown here contains 1150 free parameters. These parameters are based on coordinate product terms as described in Eq. (9) with a maximum order of 2. For a 12D system where 9 states are considered, this is an extremely simple diabatic model that serves mainly as a demonstration of the method. For an accurate model the order of the expansion will be increased in future work. However, as shown below this model is already able to give qualitatively correct PESs. There are several reasons why such a simple model is able to perform this well. The effects of the hybrid-diabatization will be discussed below. Another reason why this fairly simple model is already able to describe a large part of the nuclear configuration space is the choice of coordinates. In addition to the utilization of symmetrized coordinates, the distances of the primitive valence coordinates are transformed to tunable Morse coordinates as described elsewhere.<sup>51</sup> This allows for low order terms to already carry the properties needed for the description of the asymptotic behavior. The full details of the coordinate system used will be given in forthcoming work.

## 3. Fit results

With the diabatic model given, the next step is to obtain the diabatic PESs by optimization of the free parameters. As already mentioned above, the diagonalization of the diabatic model matrix renders the problem non-linear. Especially for big systems as is the case for the propargyl radical, the high number of free parameters becomes problematic. The convergence of the non-linear fit is very sensitive to the initial guess due to a huge number of possible local minima in the parameter space. Therefore, the direct access to the diabatic matrix elements by the block-diagonalization is utilized, which

allows us to perform *linear* least squares fits of the matrix elements individually. Although these preliminary fits do not yield good PESs, this step is very important in order to provide an optimal initial guess for this high-dimensional optimization problem. With this initial guess, it is now possible to perform a hybrid-diabatization of the available *ab initio* data.

As discussed for the other examples, another important aspect of the non-linear optimization problem is the fitting weights. However, one can easily see that the great number of *ab initio* data makes specific targeting of single fitting weights impractical. Thus, one has to choose a more general approach to determine reasonable weights. The energy weights  $\rho_{ij}$  are determined in a similar way to Eq. (20), where a simple decay model is chosen. However, the decay based on the energy difference  $\Delta_j^a = E_j^a - E_{j,ref}^a$  is amplified by a cutoff function following

$$\rho_{ij} = \left( 0.5 - \arctan \left( \frac{\alpha_1 (\Delta_j^a - \alpha_2)}{\pi} \right) \right) \cdot e^{-\alpha_3 \Delta_j^a}. \quad (26)$$

Here,  $\alpha_1 = 30$ ,  $\alpha_2 = 0.2$ , and  $\alpha_3 = 8$  are system-specific parameters that can be adapted as suitable. The focus on the differences with respect to the reference energies allows for the inner region close to the  $C_{2v}$  minimum to be described very well and the outer regions to be represented with sufficient accuracy. For the results shown the weights of the CI coefficients are scaled to be 0.1% of the weights of the energies. This concept is still preliminary for the propargyl radical and may be adapted to a more advanced model in future work.

The fitting results shown in the following are based on 3601 geometry points. The 9 adiabatic states considered yield 32 409 *ab initio* energies. Despite this large number, one can easily see that the sampling is still very sparse for a proper representation of a 12D nuclear configuration space. In contrast to a diabaticization by *ansatz*, the hybrid-diabatization offers a way to increase the information content for the non-linear optimization. As already discussed above, this is achieved by inclusion of the CI coefficients, yielding another 324 090 data. Here lies a great strength of the hybrid-diabatization. As discussed above, the block-diagonalization data already allow for a physically motivated diabatic model and help by improving the convergence of the optimization problem. In the same manner, these data are now used to reduce the effects of undersampling one has to face in the construction of high-dimensional PESs. The adiabatic wavefunctions are very well suited for this task, as they may already contain information that would normally require the calculation of more data points. In addition to this, the effects one can see at conical intersections or avoided crossings are typically better described by the CI coefficients than by the energies. The requirement of the non-linear fit to correctly reproduce the adiabatic wavefunctions ensures that the diabatic model describes the physics in such regions properly, especially the rapid changes in the adiabatic state compositions. The price to pay is that the non-linear optimization may not yield the best rms errors concerning the energies. However, the advantages greatly surpass the disadvantages in this regard, which is especially important for systems with many complicated state interactions like methyl iodide or the propargyl radical.

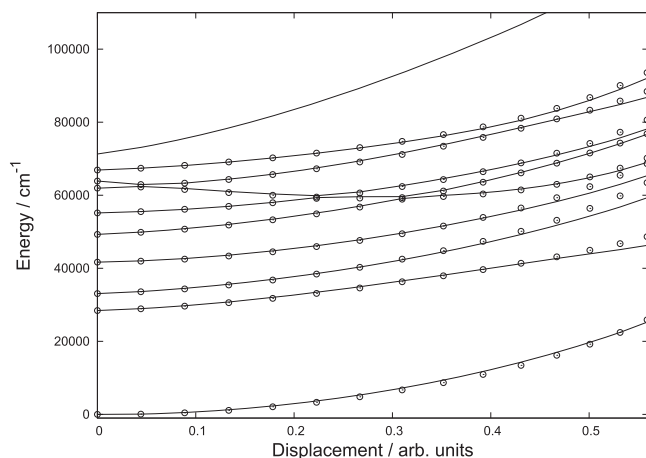


FIG. 9. Results obtained by the hybrid-diabatization along a 12D random cut through the PESs of propargyl. Open circles are *ab initio* energies and the solid lines are the adiabatic energies obtained by the hybrid-diabatization.

Overall, the fitting results for propargyl are in good agreement with the *ab initio* data and the rms error of the non-linear fit amounts to  $483.7\text{ cm}^{-1}$ . Representative results for the adiabatic energies obtained by the hybrid-diabatization are presented in Figures 9 and 10. Open circles are the *ab initio* energies and the solid lines are the adiabatic energies obtained by the hybrid-diabatization.

For both examples, it is observed that the region near the reference point of the model is described extremely well. Farther away from the origin the agreement becomes less good as expected. On the one hand, this can be explained by the used weights as discussed above, where the weights are based on the differences of the reference energies at each geometry point. On the other hand, the model used in this example is the simplest possible approximation to get a qualitatively correct description of the PESs. There is still a lot of room for improvement and corresponding work is currently in progress.

The first example given in Figure 9 focuses on the description of the state interactions. Here, the most interesting aspect is the state interactions among the states 5–8. This interaction is described very well with only small deviations in state 7 after the crossing. The next interactions occur at around 0.23 and 0.31 and both show avoided crossings between the states.

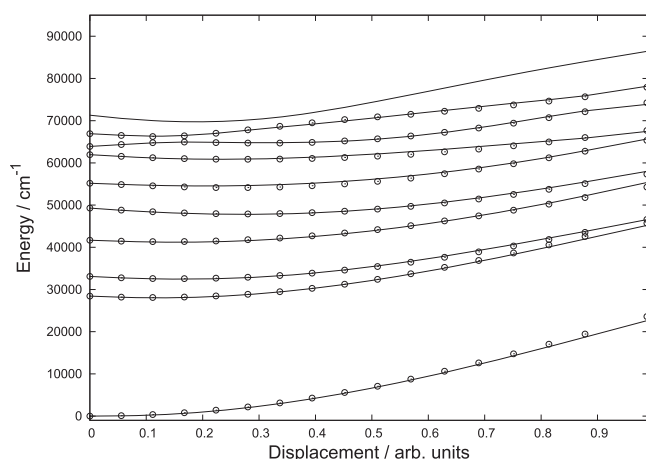


FIG. 10. Results obtained by the hybrid-diabatization along a 12D random cut through the PESs of propargyl. The color coding is the same as in Figure 9.

These interactions are also well described with only small deviations. In this particular example, the utilization of the virtual state (highest model adiabatic data) does not seem to be needed. One can easily see that the virtual state does not interfere with the other adiabatic states at all. However, the electronic structure may change for different regions in the nuclear configuration space. This becomes clear by considering the next example in Figure 10. It is easy to see that the virtual state is important for the description of the state interactions. States 8 and 9 show an avoided crossing around 0.16, which is described well. By the shape of state 9 at around 0.4, it quickly becomes clear that another state is needed to describe this region. However, there are no *ab initio* data available. In this case the information of the adiabatic wave functions is used to simulate the avoided crossing with the next higher state. This actually is key for the ability to diabaticize the reference data reasonably. One can argue that it is possible to describe such behavior by introducing a more flexible diabatic model. This approach may very well lead to a reasonable rms error, however, the focus should always lie on the physics of the system. The introduction of the virtual state does exactly this. By adding the missing diabatic state and the utilization of the adiabatic wave functions as extra information, one can achieve good fitting results even with a simple diabatic model and represent the physics correctly. This is of great advantage when applying our method to different molecules of larger size. A more flexible model always goes hand in hand with a higher number of parameters that need to be optimized. As one can see, even for a simple model, the number of parameters needed to describe the electronic structure of the propargyl radical is quite high.

#### IV. CONCLUSIONS

A new method for the diabaticization of adiabatic electronic energies and wave functions and the development of accurate diabatic potential energy surfaces (PESs) has been developed. In this method adiabatic wave function information is used simultaneously with adiabatic energy data and both are required to be reproduced by a parametrized diabatic model Hamiltonian. This can be considered a combination of block-diagonalization and diabaticization by *ansatz* approaches and thus is called *hybrid diabaticization*. The new method overcomes a number of disadvantages of previous approaches. Other than pure block-diagonalization approaches, it yields analytic diabatic PESs directly and in contrast to standard diabaticization by *ansatz* techniques the reproduction of the adiabatic wave functions ensures physically meaningful results.

In a first step, the adiabatic states and wave functions of interest are analysed and the diabatic state space required to represent all relevant adiabatic states in the region of interest is determined. The diabatic states are characterized by their wave functions (typically CSF coefficients) at a chosen reference point. Then for each point in nuclear configuration space, the adiabatic wave functions are projected onto this diabatic state space and orthonormalized like in typical block-diagonalization approaches. In the second step, a parametrized diabatic model matrix of the dimension of the diabatic state space is setup. In this step the block-diagonalization data can



be utilized to develop an optimal diabatic model. Finally, the parameters of the diabatic model are determined by fitting the adiabatic energy data and projected wave function data, which have to be reproduced in a least-squares sense by the eigenvalues and eigenvectors of the diabatic model. The non-linear fitting benefits greatly from an initial guess that can be generated by a preliminary fit of the single matrix elements from the block-diagonalization data.

The new approach has a number of advantageous features. For systems beyond three atoms the sampling of the nuclear configuration space for the generation of reference data becomes increasingly sparse. The utilization of the wave function data increases the information content of each data point considerably, thus reducing the arbitrariness due to the under-sampling. The requirement of the diabatic model to reproduce adiabatic energies as well as wave functions also ensures that the result is much more reliable than a standard diabatization by *ansatz*. Diabatic wave functions and properties can be obtained in this way, which are of high quality and really represent the physics of the system. We utilize this capability, e.g., in the ERCAR method developed by us in order to generate very accurate fine structure state PESs from simple non-relativistic *ab initio* data and experimental atomic spin-orbit data combined with a specific hybrid diabatization. In that context, a further feature of the hybrid diabatization is highly relevant. It allows in a straightforward way to represent a system by a diabatic model of higher dimensionality than the number of adiabatic states available as reference data. This is necessary for the ERCAR method for the modeling of the spin-orbit effects but also for non-relativistic systems whenever the highest adiabatic state shows avoided crossings with states not included in the reference data. Especially the latter is a very common and tough problem in the development of excited state PESs and now can be treated by hybrid diabatization.

The different features and the power of our new method are demonstrated by three examples. First we present as proof-of-principle application the diabatization of the  $^1A_1$  and  $^1B_2$  electronic states of ozone in the region of their conical intersection. The chosen two-dimensional two-state problem has been utilized before by other groups for this purpose. Our results show that the hybrid diabatization is capable of yielding analytic diabatic PESs of excellent accuracy with an rms with respect to the reference energy data of about  $4\text{ cm}^{-1}$ . The error of the PES model is significantly lower than that obtained from a comparable fit using the same model and the pure block-diagonalization data, showing the power of the hybrid diabatization. The second application is the one-dimensional diabatization of a large number of adiabatic states of methyl iodide,  $\text{CH}_3\text{I}$ . The breaking of the C-I bond is modeled, which induces drastic changes in the electronic structure. This case demonstrates the handling of adiabatic intruder states which require a diabatic state basis larger than the number of available adiabatic states. This example also is used to investigate the influence of the data weighting during the non-linear fitting, which turns out to be important. Again, a diabatic model of excellent accuracy is obtained with final rms errors for energies between  $7$  and  $23\text{ cm}^{-1}$  and below  $2\%$  of squared CI coefficients for the projected wave functions. As a final application,

we present a 12-dimensional diabatic model for 9 adiabatic states of the propargyl radical. This example demonstrates the capability to handle high-dimensional problems with many electronic states. The electronic structure of this system is very complicated with numerous avoided crossings and conical intersections including intruder states. In this case the 9 adiabatic states can be represented by 10 diabatic states, which becomes possible by the hybrid diabatization. Due to the high dimensionality and the large state space, only the simplest diabatic model is fitted so far and the rms error of the energies is still  $484\text{ cm}^{-1}$ . Nevertheless, this is a very promising result and shows the capacity of the hybrid diabatization. The numerical result will be improved by developing a more advanced model in the near future and corresponding work currently is in progress.

## ACKNOWLEDGMENTS

We are grateful to the Deutsche Forschungsgemeinschaft (DFG) for generous financial support. Calculations leading to the results presented here were performed on resources provided by the Paderborn Center for Parallel Computing.

- <sup>1</sup>M. A. Collins and D. F. Parsons, *J. Chem. Phys.* **99**, 6756 (1993).
- <sup>2</sup>J. Ischtwan and M. A. Collins, *J. Chem. Phys.* **100**, 8080 (1994).
- <sup>3</sup>T. S. Ho and H. Rabitz, *J. Chem. Phys.* **104**, 2584 (1996).
- <sup>4</sup>G. G. Maisuradze, D. L. Thompson, A. F. Wagner, and M. Minkoff, *J. Chem. Phys.* **119**, 10002 (2003).
- <sup>5</sup>G. G. Maisuradze, A. Kawano, D. L. Thompson, A. F. Wagner, and M. Minkoff, *J. Chem. Phys.* **121**, 10329 (2004).
- <sup>6</sup>B. J. Braams and J. M. Bowman, *Int. Rev. Phys. Chem.* **28**, 577 (2009).
- <sup>7</sup>T. B. Blank, S. D. Brown, A. W. Calhoun, and D. J. Doren, *J. Chem. Phys.* **103**, 4129 (1995).
- <sup>8</sup>D. F. Brown, M. N. Gibbs, and D. C. Clary, *J. Chem. Phys.* **105**, 7597 (1996).
- <sup>9</sup>K. T. No, B. H. Chang, S. Y. Kim, M. S. Jhon, and H. A. Scheraga, *Chem. Phys. Lett.* **271**, 152 (1997).
- <sup>10</sup>F. V. Prudente, P. H. Acioli, and J. J. S. Neto, *J. Chem. Phys.* **109**, 8801 (1998).
- <sup>11</sup>S. Lorenz, A. Gross, and M. Scheffler, *Chem. Phys. Lett.* **395**, 210 (2004).
- <sup>12</sup>L. M. Raff, M. Malshe, M. Hagan, D. I. Doughan, M. G. Rockley, and R. Komanduri, *J. Chem. Phys.* **122**, 084104 (2005).
- <sup>13</sup>S. Lorenz, M. Scheffler, and A. Gross, *Phys. Rev. B* **73**, 115431 (2006).
- <sup>14</sup>S. Manzhos, X. G. Wang, R. Dawes, and T. Carrington, *J. Phys. Chem. A* **110**, 5295 (2006).
- <sup>15</sup>S. Manzhos and T. Carrington, Jr., *J. Chem. Phys.* **125**, 084109 (2006).
- <sup>16</sup>S. Manzhos and T. Carrington, Jr., *J. Chem. Phys.* **125**, 194105 (2006).
- <sup>17</sup>J. Behler and M. Parrinello, *Phys. Rev. Lett.* **98**, 146401 (2007).
- <sup>18</sup>S. Manzhos and T. Carrington, Jr., *J. Chem. Phys.* **127**, 014103 (2007).
- <sup>19</sup>M. Malshe, R. Narulkar, L. M. Raff, M. Hagan, S. Bukkapatnam, and R. Komanduri, *J. Chem. Phys.* **129**, 044111 (2008).
- <sup>20</sup>S. Manzhos and T. Carrington, Jr., *J. Chem. Phys.* **129**, 224104 (2008).
- <sup>21</sup>J. Behler, *J. Chem. Phys.* **134**, 074106 (2011).
- <sup>22</sup>H. T. T. Nguyen and H. M. Le, *J. Phys. Chem. A* **116**, 4629 (2012).
- <sup>23</sup>B. Jiang, J. Li, and H. Guo, *Int. Rev. Phys. Chem.* **35**, 479 (2016).
- <sup>24</sup>W. Koch and D. H. Zhang, *J. Chem. Phys.* **141**, 021101 (2014).
- <sup>25</sup>C. R. Evenhuis and M. A. Collins, *J. Chem. Phys.* **121**, 2515 (2004).
- <sup>26</sup>C. R. Evenhuis, X. Lin, D. H. Zhang, D. Yarkony, and M. A. Collins, *J. Chem. Phys.* **123**, 134110 (2005).
- <sup>27</sup>O. Godsi, C. R. Evenhuis, and M. A. Collins, *J. Chem. Phys.* **125**, 104105 (2006).
- <sup>28</sup>H. Guo and D. R. Yarkony, *Phys. Chem. Chem. Phys.* **18**, 26335 (2016).
- <sup>29</sup>C. Xie, J. Ma, X. Zhu, D. H. Zhang, D. R. Yarkony, D. Xie, and H. Guo, *J. Phys. Chem. Lett.* **5**, 1055 (2014).
- <sup>30</sup>*Conical Intersections: Electronic Structure, Dynamics and Spectroscopy*, edited by W. Domcke, D. R. Yarkony, and H. Köppel (World Scientific, Singapore, 2004).
- <sup>31</sup>H. C. Longuet-Higgins, *Adv. Spectrosc.* **2**, 429 (1961).
- <sup>32</sup>W. Lichten, *Phys. Rev.* **131**, 229 (1963).

- <sup>33</sup>W. Lichten, *Phys. Rev.* **164**, 131 (1967).  
<sup>34</sup>F. T. Smith, *Phys. Rev.* **179**, 111 (1969).  
<sup>35</sup>M. Baer, *Chem. Phys.* **15**, 49 (1976).  
<sup>36</sup>H. Werner and W. Meyer, *J. Chem. Phys.* **74**, 5802 (1981).  
<sup>37</sup>C. A. Mead and D. G. Truhlar, *J. Chem. Phys.* **77**, 6090 (1982).  
<sup>38</sup>C. A. Mead, *J. Chem. Phys.* **78**, 807 (1983).  
<sup>39</sup>H.-J. Werner, B. Follmeg, and M. H. Alexander, *J. Chem. Phys.* **89**, 3139 (1988).  
<sup>40</sup>T. Pacher, L. S. Cederbaum, and H. Köppel, *J. Chem. Phys.* **89**, 7367 (1988).  
<sup>41</sup>T. Pacher, C. A. Mead, L. S. Cederbaum, and H. Köppel, *J. Chem. Phys.* **91**, 7057 (1989).  
<sup>42</sup>T. Pacher, H. Köppel, and L. S. Cederbaum, *J. Chem. Phys.* **95**, 6668 (1991).  
<sup>43</sup>T. Pacher, L. S. Cederbaum, and H. Köppel, *Adv. Chem. Phys.* **84**, 293 (1993).  
<sup>44</sup>H. Köppel, W. Domcke, and L. S. Cederbaum, *Adv. Chem. Phys.* **57**, 59 (1984).  
<sup>45</sup>A. J. C. Varandas, F. B. Brown, C. A. Mead, D. G. Truhlar, and N. C. Blais, *J. Chem. Phys.* **86**, 6258 (1987).  
<sup>46</sup>A. Viel and W. Eisfeld, *J. Chem. Phys.* **120**, 4603 (2004).  
<sup>47</sup>W. Eisfeld and A. Viel, *J. Chem. Phys.* **122**, 204317 (2005).  
<sup>48</sup>A. Viel, W. Eisfeld, S. Neumann, W. Domcke, and U. Manthe, *J. Chem. Phys.* **124**, 214306 (2006).  
<sup>49</sup>A. Viel, W. Eisfeld, C. R. Evenhuis, and U. Manthe, *Chem. Phys.* **347**, 331 (2008).  
<sup>50</sup>S. Faraji, H. Köppel, W. Eisfeld, and S. Mahapatra, *Chem. Phys.* **347**, 110 (2008).  
<sup>51</sup>W. Eisfeld, O. Vieuxmaire, and A. Viel, *J. Chem. Phys.* **140**, 224109 (2014).  
<sup>52</sup>G. Hirsch, R. J. Buenker, and C. Petrongolo, *Mol. Phys.* **70**, 835 (1990).  
<sup>53</sup>R. Cimiraglia, J. P. Malrieu, M. Persico, and F. Spiegelmann, *J. Phys. B: At. Mol. Phys.* **18**, 3073 (1985).  
<sup>54</sup>W. Domcke and C. Woywod, *Chem. Phys. Lett.* **216**, 362 (1993).  
<sup>55</sup>W. Domcke, C. Woywod, and M. Stengle, *Chem. Phys. Lett.* **226**, 257 (1994).  
<sup>56</sup>G. J. Atchity and K. Ruedenberg, *Theor. Chem. Acc.* **97**, 47 (1997).  
<sup>57</sup>R. Sadygov and D. Yarkony, *J. Chem. Phys.* **109**, 20 (1998).  
<sup>58</sup>H. Nakamura and D. G. Truhlar, *J. Chem. Phys.* **115**, 10353 (2001).  
<sup>59</sup>H. Nakamura and D. G. Truhlar, *J. Chem. Phys.* **117**, 5576 (2002).  
<sup>60</sup>R. Abrol and A. Kuppermann, *J. Chem. Phys.* **116**, 1035 (2002).  
<sup>61</sup>H. Nakamura and D. G. Truhlar, *J. Chem. Phys.* **118**, 6816 (2003).  
<sup>62</sup>M. S. Schuurman and D. R. Yarkony, *J. Chem. Phys.* **127**, 094104 (2007).  
<sup>63</sup>B. N. Papas, M. S. Schuurman, and D. R. Yarkony, *J. Chem. Phys.* **129**, 124104 (2008).  
<sup>64</sup>X. Zhu and D. R. Yarkony, *J. Chem. Phys.* **130**, 234108 (2009).  
<sup>65</sup>X. Zhu and D. R. Yarkony, *J. Chem. Phys.* **132**, 104101 (2010).  
<sup>66</sup>X. Zhu and D. R. Yarkony, *J. Chem. Phys.* **136**, 174110 (2012).  
<sup>67</sup>H. Lischka, M. Dallos, P. G. Szalay, D. R. Yarkony, and R. Shepard, *J. Chem. Phys.* **120**, 7322 (2004).  
<sup>68</sup>R. Valero and D. G. Truhlar, *J. Phys. Chem. A* **111**, 8536 (2007).  
<sup>69</sup>C. Woywod, M. Stengle, W. Domcke, H. Flothmann, and R. Schinke, *J. Chem. Phys.* **107**, 7282 (1997).  
<sup>70</sup>H. Ndome, R. Welsch, and W. Eisfeld, *J. Chem. Phys.* **136**, 034103 (2012).  
<sup>71</sup>H. Ndome and W. Eisfeld, *J. Chem. Phys.* **137**, 064101 (2012).  
<sup>72</sup>N. Wittenbrink, H. Ndome, and W. Eisfeld, *J. Phys. Chem. A* **117**, 7408 (2013).  
<sup>73</sup>K. Ruedenberg and G. J. Atchity, *J. Chem. Phys.* **99**, 3799 (1993).  
<sup>74</sup>J. Hendekovic, *Chem. Phys. Lett.* **90**, 193 (1982).  
<sup>75</sup>F. X. Gadea and M. Pelissier, *J. Chem. Phys.* **93**, 545 (1990).  
<sup>76</sup>B. Heumann, K. Weide, R. Dören, and R. Schinke, *J. Chem. Phys.* **98**, 5508 (1993).  
<sup>77</sup>W. Domcke, A. L. Sobolewski, and C. Woywod, *Chem. Phys. Lett.* **203**, 220 (1993).  
<sup>78</sup>D. Opalka and W. Domcke, *Chem. Phys. Lett.* **494**, 134 (2010).  
<sup>79</sup>D. Opalka and W. Domcke, *J. Chem. Phys.* **132**, 154108 (2010).  
<sup>80</sup>F. Venghaus and W. Eisfeld, *J. Chem. Phys.* **144**, 114110 (2016).  
<sup>81</sup>A. Szabo and N. S. Ostlund, *Modern Quantum Chemistry* (McGraw Hill, New York, 1982).  
<sup>82</sup>H.-J. Werner, P. J. Knowles, G. Knizia, F. R. Manby, M. Schütz, P. Celani, T. Korona, R. Lindh, A. Mitrushenkov, G. Rauhut, K. R. Shamasundar, T. B. Adler, R. D. Amos, A. Bernhardsson, A. Berning, D. L. Cooper, M. J. O. Deegan, A. J. Dobbyn, F. Eckert, E. Goll, C. Hampel, A. Hesselmann, G. Hetzer, T. Hrenar, G. Jansen, C. Köppl, Y. Liu, A. W. Lloyd, R. A. Mata, A. J. May, S. J. McNicholas, W. Meyer, M. E. Mura, A. Nicklass, D. P. O'Neill, P. Palmieri, D. Peng, K. Pflüger, R. Pitzer, M. Reiher, T. Shiozaki, H. Stoll, A. J. Stone, R. Tarroni, T. Thorsteinsson, and M. Wang, *MOLPRO*, version 2012.1, a package of *ab initio* programs, 2012, see <http://www.molpro.net>.  
<sup>83</sup>H.-J. Werner and P. J. Knowles, *J. Chem. Phys.* **89**, 5803 (1988).  
<sup>84</sup>P. J. Knowles and H.-J. Werner, *Chem. Phys. Lett.* **145**, 514 (1988).  
<sup>85</sup>W. Eisfeld, *Phys. Chem. Chem. Phys.* **7**, 3924 (2005).  
<sup>86</sup>W. Eisfeld, *J. Phys. Chem. A* **110**, 3903 (2006).